



ISSN: 0067-2904

## Optimization of photoluminescence properties of Porous silicon by adding gold nanoparticles

Alwan M. Alwan<sup>1\*</sup>, Intisar A. Naseef<sup>2</sup>

<sup>1</sup> School of Applied Science, University of Technology, Baghdad, Iraq.

<sup>2</sup> Ministry of Science and Technology, Baghdad, Iraq.

### Abstract

In this work, the photoluminescence spectra (PL) of porous silicon (PS) have been modified by adding gold nanoparticles (AuNPs) to PS layer. PS was produced via Photo electro-chemical etching (PECE) method of n-type Si wafer with resistivity of about (10  $\Omega$ .cm) and (100) orientation. Laser wavelength of (630 nm) and illumination intensity of about (30 mW/cm<sup>2</sup>), etching current density of (10mA/cm<sup>2</sup>), and etching time of (4 min) were used during the etching process. The bare PS before metallic deposition process and porous silicon/gold nanoparticles (PS/AuNPs) structures were investigated by X-Ray Diffraction (XRD), scanning electron microscopy (SEM), and energy dispersive X-Ray (EDX). The photoluminescence spectra were investigated as a function of gold nanoparticles sizes and distribution on the surface of PS.

It was found that there are two behaviours were observed for the photoluminescence spectra of PS/AuNPs substrate; quenching and enhancement effects based on the average gold nanoparticles sizes and their aggregation forms.

**Keywords:** PS/AuNPs, PECE process, HF acid, Photoluminescence spectra, gold nanoparticles, metallic solution concentration.

## تحسين خصائص التلؤلؤ الضوئي للسليكون المسامي باضافة جسيمات الذهب النانوية

علوان محمد علوان<sup>1\*</sup>، انتصار علي نصيف<sup>2</sup>

<sup>1</sup> قسم العلوم التطبيقية، الجامعة التكنولوجية، بغداد، العراق.

<sup>2</sup> وزارة العلوم والتكنولوجيا، بغداد، العراق.

### الخلاصة

في هذا البحث تم تحسين طيف التلؤلؤ الضوئي للسليكون المسامي عن طريق اضافة جسيمات الذهب النانوية الى طبقة السليكون المسامي. السليكون المسامي تم تحضيره بطريقة التتميش الضوء كهروكيميائية لشريحة السليكون من النوع المانح ذات مقاومة (10) اوم.سم وتوجه (100). الليزر ذو الطول الموجي (630) نانومتر بشدة اضاءة (30) ملي واط ا سم<sup>2</sup>، وكثافة تيار التتميش (10) ملي امبيراً سم<sup>2</sup>، وزمن تتميش (4) دقائق تم استخدامها خلال عملية التتميش. تراكيب السليكون المسامي المجرى (قبل عملية الترسب المعدني) والسليكون المسامي المطعم بجسيمات الذهب النانوية تم دراستها بواسطة قياس حيود الاشعة السينية، المجهر الماسح الالكتروني، وقياس تشتت طاقة الاشعة السينية. طيف اللمعان الضوئي تم دراسته كدالة لحجم جسيمات الذهب النانوية وتوزيعها على سطح السليكون المسامي. لقد وجد ان هناك سلوكين تم ملاحظتهما بالنسبة لطيف اللمعان الضوئي لتراكيب السليكون المسامي المطعم بجسيمات الذهب النانوية: هما ظاهرتي الاخامد والتعزيز بناء على معدل حجم جسيمات الذهب النانوية واشكال تكتلاتها.

## 1) Introduction

Porous silicon (PS) exhibits exceptional physical and chemical features as compared to crystalline silicon due to the quantum confinement effect. The effective visible photoluminescence (PL) presents one of the most significant effects which intensely affected by huge surface of the porous matrix [1]. Quantum Confinement effects in PS and the possibility of the recombination of the electrons and holes is greater in low-dimensional PS leading to high emission efficiency due to the high porosity structures of porous silicon where the material's band gap is converted from indirect to direct band gap. This change of band gap arises as the nanoscale system and the conversion is controlled by many factors like porosity, surface passivation, pore size and size distribution [2]. The surface morphology of PS can be improved by incorporating metallic nanoparticles since the adjustability of the porous surface properties, such as roughness and pores size control the size of metal nanoparticles. The morphology and the size of metal nanoparticles were found to be affected by the PS pore (size and shape), and surface roughness at the same immersion conditions [3].

The reaction between the adding nanoparticles and the inner surface of PS matrix can modify the luminescence by inhibiting and degrading the non-radiative recombination processes [4]. The pores on PS surface perform as binding locations attracting foreign species to be adsorbed on the spongy structure of PS [5]. Metals such as Cu, Ag, and Au have also been used to modify the surface of PS and develop more stable photoluminescence properties [6].

**Meddeb Hosny (et al. )** [6] studied the effects of the size, morphology and distribution of gold colloid on porous silicon characteristics. The photoluminescence (PL) spectroscopy revealed that the PL intensity strongly depends on gold nanoparticles deposition which is accredited to the small size of metal nanoparticles that equally coated the surface. It was also observed that the phenomenon of visible light emission isn't an intrinsic property of silicon, but it is highly dependent on chemical reactions of silicon with hydrogen and oxygen. While **M-B Bouzouraa (et al. )** [7] studied the modification of PL spectra for porous silicon layer by adding Cobalt nanoparticles to form (PS/Co) composites which is deposited at different etching times. They concluded that the highest PL spectra were perceived for immersion duration of 60 min. while the amount of deposited cobalt in the case of long deposition times acts as a trap and stimulates the non-radiative energy transfer leading to quench the PL spectra.

In this paper, we investigated the effect of gold nanoparticles sizes and morphology on the behavior of PL spectra of PS/AuNPs structure and discussed the variations of PL spectra based on the X-Ray Diffraction patterns, and SEM image analyzes of gold nanoparticles.

## 2. Experimental work

### 2.1) chemical materials

Hydrofluoric acid 48%, (CDH), India, was used and diluted with high purity ethanol 99.8%,(SIGMA-ALDRICH, Germany) to prepare the required concentration for the etching solutions of about 24% HF. Hydrogen tetrachlorocuprate (III) (HAuCl<sub>4</sub>) (Aldrich, 99.99%) and their mixtures with HF acid at different concentrations were used to deposit the surface of PS. The required solution concentrations were prepared using the following equation [8]:

$$\text{Molarity} = \frac{w}{\frac{M.Wt}{V}} \dots\dots\dots (1)$$

where W (gm.) is the weight of the H<sub>2</sub>AuCl<sub>4</sub>, M.Wt (gm. /mole) is the molecular weight, and V is the volume of the dissolved solution.

### 2.2) PS preparation

PS samples were prepared by Photo electro-chemical etching (PECE) process at room temperature from n-type (100) oriented Si substrates having a resistivity of (10 Ω.cm). Si substrates have been cut out into pieces with area of (2x2) cm<sup>2</sup>, and then washed in (HF: ethanol= 1:10) mixture to eliminate the SiO<sub>2</sub> layer, then kept in methanol to prevent the oxidization of the samples. A cell made of Teflon was used for the etching process. The etching solution is (1:1) mixture of hydrofluoric acid (HF) of concentration (24%) and ethanol (C<sub>2</sub>H<sub>5</sub>OH). laser of wavelength (630) nm and fixed output power density of about (30 mW/cm<sup>2</sup>) was the illumination source employed in this study.

In PECE process, Si represents the anode and the platinum ring represents the cathode. The etching time is (4min) and current density is about (10 mA/cm<sup>2</sup>).The illuminated area is about (1cm<sup>2</sup>).Figure-1 below shows the schematic diagram of PECE process.

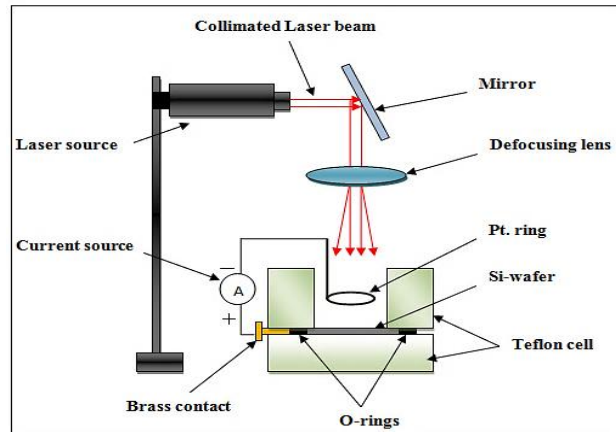


Figure 1- schematic diagram of PECE process.

### 2.3) gold nanoparticles deposition process

PS substrates were deposited with the gold nanoparticles solution at fixed time of (5 min) via the immersion plating method in dark room. The deposition of PS samples was carried for different concentrations of ( $\text{HAuCl}_4$ ) solution with HF additive acid of about ( $10^{-2}\text{M}$ ,  $10^{-2}\text{M}$  diluted in 2.9 M of HF,  $5 \times 10^{-3}\text{M}$ , and  $5 \times 10^{-3}\text{M}$  diluted in 2.9 M of HF) to form PS/AuNPs structure due to the reduction process. AuNPs were created naturally as given in the equations [9]:



The immersion plating method presents a special technique based on the galvanic displacement reaction in which cathodic reaction and anodic reaction happen at the same time [10]. It represents a desirable approach since it doesn't require any electrodes or any external source of electricity to deposit a metal, its simplicity and easy conduct. Also, it doesn't require vacuum technologies or energy source [11].

### 2.4) characterization

The structural properties of bare PS and PS/AuNPs structures were investigated via X-Ray Diffraction analysis using a high resolution X-ray device (XRD 6000 shimadzu). The X-ray source incorporates copper which emits its radiation at wavelength of at (0.154 nm).

Image-J software was used to calculate the statistical distribution of pore sizes and AuNPs sizes based on SEM images analysis, while the PL spectra measurement was carried out by exciting the PS samples with (He-Cd) laser at a wavelength of (325 nm) in order to excite the almost range of Si crystallites which contribute in the PL spectra. The PL spectra were examined by (LiCuix 3205 N) system in addition to the EDX analysis that confirms the existence of AuNPs on PS surface.

## 3) Results and discussion

### 3.1) Structural Measurements

The XRD patterns of bare PS and PS/AuNPs samples are illustrated in Figures -2 and 3 respectively. All diffraction peaks were assigned according to the standards powder diffraction card of Joint Committee on Powder Diffraction standards (JCPDS).

From Figure-2, the diffraction patterns of bare PS layer shows that the porous layer stills crystalline in the plane (100) at ( $2\theta$ ) diffraction angle of about ( $32.4^\circ$ ).

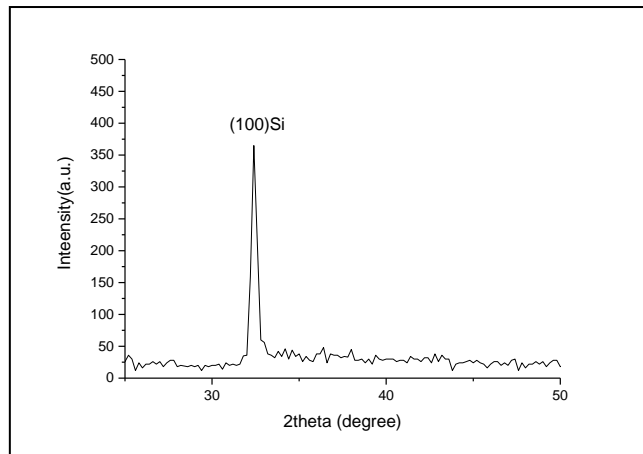


Figure 2- Shows the XRD patterns of bare PS layer.

The XRD patterns for PS/AuNPs structure deposited with (HAuCl<sub>4</sub>) at concentrations of (10<sup>-2</sup> M, 10<sup>-2</sup> M diluted in HF, 5x10<sup>-3</sup> M, and 5x10<sup>-3</sup> M diluted in HF) respectively are shown in Figure- 3a,b,c,d.

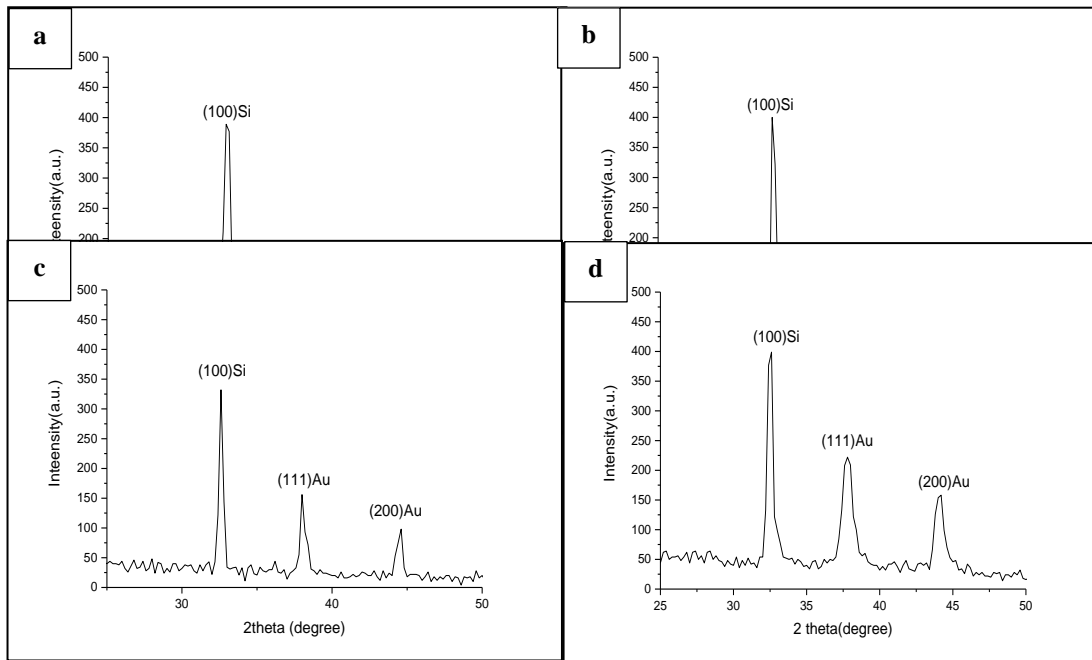


Figure 3- The XRD patterns of hybrid structure PS/AuNPs deposited with HAuCl<sub>4</sub> at concentrations of: a) 10<sup>-2</sup> M b) 10<sup>-2</sup> M diluted in HF c) 5x10<sup>-3</sup> M d) 5x10<sup>-3</sup> M diluted in HF.

Scherer's formula was used to calculate the size of AuNPs (D<sub>p</sub>) as follows [12]:

$$D_p = \frac{0.9\lambda}{\beta \cos\theta} \dots \dots \dots (4)$$

Table -1 ,shows the obtained numerical data including the experimental values of diffraction angles at different concentrations of HAuCl<sub>4</sub>. While Table -2 shows the values of FWHM, size of AuNPs, and S.S.A. of AuNPs, respectively.

**Table 1-** The standard and experimental diffraction angles of AuNPs for PS/AuNPs structure.

HAuCl <sub>4</sub> concentration(M)	2θ in degree at the plane (111) (Standard =38.100°) <b>experimental</b>	2θ in degree at the plane (200) (Standard =44.369°) <b>experimental</b>
10 <sup>-2</sup>	<b>38.2</b>	<b>44.4</b>
10 <sup>-2</sup> + HF	<b>38.4</b>	<b>43.6</b>
5x10 <sup>-3</sup>	<b>38</b>	<b>44.6</b>
5x10 <sup>-3</sup> +HF	<b>37.8</b>	<b>44</b>

**Table 2-** The FWHM, the size and specific surface area(S.S.A.) of AuNPs for PS/AuNPs structure.

HAuCl <sub>4</sub> concentration (M)	Plane (111)			plane (200)		
	FWHM (rad)	Size of AuNPs (nm)	S.S.A of AuNPs (m <sup>2</sup> /gm)	FWHM (rad)	Size of AuNPs (nm)	S.S.A of AuNPs (m <sup>2</sup> /gm)
10 <sup>-2</sup>	<b>0.004</b>	<b>34.6</b>	<b>9</b>	<b>0.0034</b>	<b>40.78</b>	<b>7.62</b>
10 <sup>-2</sup> +HF	<b>0.006</b>	<b>23</b>	<b>13.5</b>	<b>0.0052</b>	<b>26.66</b>	<b>11.66</b>
5x10 <sup>-3</sup>	<b>0.0087</b>	<b>15.9</b>	<b>19.55</b>	<b>0.0157</b>	<b>8.83</b>	<b>35.2</b>
5x10 <sup>-3</sup> +HF	<b>0.017</b>	<b>8.15</b>	<b>38.14</b>	<b>0.019</b>	<b>7.3</b>	<b>42.64</b>

From Table -1 , it can be seen that there is a little change in diffraction angles (2θ) or interaction space, this change is due to the presence of local microscopic deformation strain (Microscopic deformation i.e. local variation of inter atomic distance of metal nanoparticles) for AuNPs/PS structure samples which is also referred to as a microstrain [13]. In the same manner, the decrease of grain sizes values and the increase of S.S.A. values for AuNPs are shown in Table -2 is due to the fact that gold formation depends on morphology of porous layer and the effect of HAuCl<sub>4</sub> concentration. These results agrees with those obtained from [12].

**3.2) Morphological Measurements:**

Figure -4 illustrates the SEM image of the surface morphology of bare PS layer.

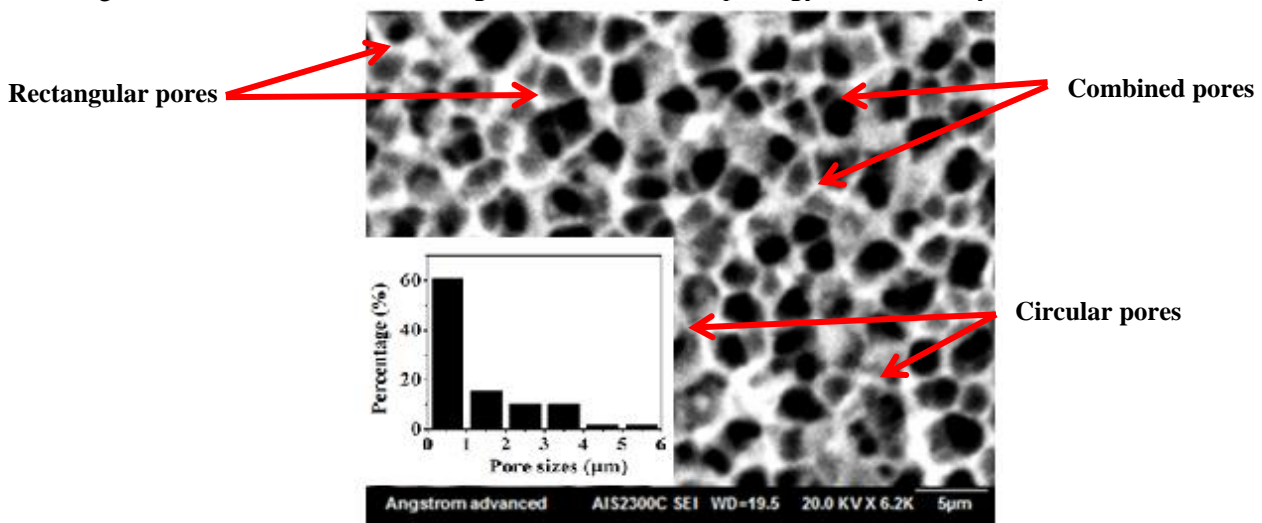


**Figure 4-** The SEM images of bare PS with the statistical distribution of pore size.

The pore-like structure of bare PS with pores shapes nearly cylindrical, rectangular, and combined are presented. The statistical distribution of the pore size shows that the pore size distribution is nonsymmetrical. The pores sizes range from (0.5 – 6)  $\mu\text{m}$  and the peak of the distribution is located at (0.5 $\mu\text{m}$ ).

The variation in the pore size across the PS layer surface may be due to the Gaussian distribution of the illumination intensity, where the maximum intensity is at the center and the minimum at the edge of the laser spot size. So, this will produce nonsymmetrical etching rate on the surface.

Figure -5 shows the SEM images of PS/AuNPs structure resulted from depositing the surface of PS with hydrogen tetrachlorocuprate ( $\text{HAuCl}_4$ ) solution with different concentrations. This figure shows different morphologies of AuNPs in addition to the statistical distribution of AuNPs sizes as a function of ( $\text{HAuCl}_4$ ) concentration.

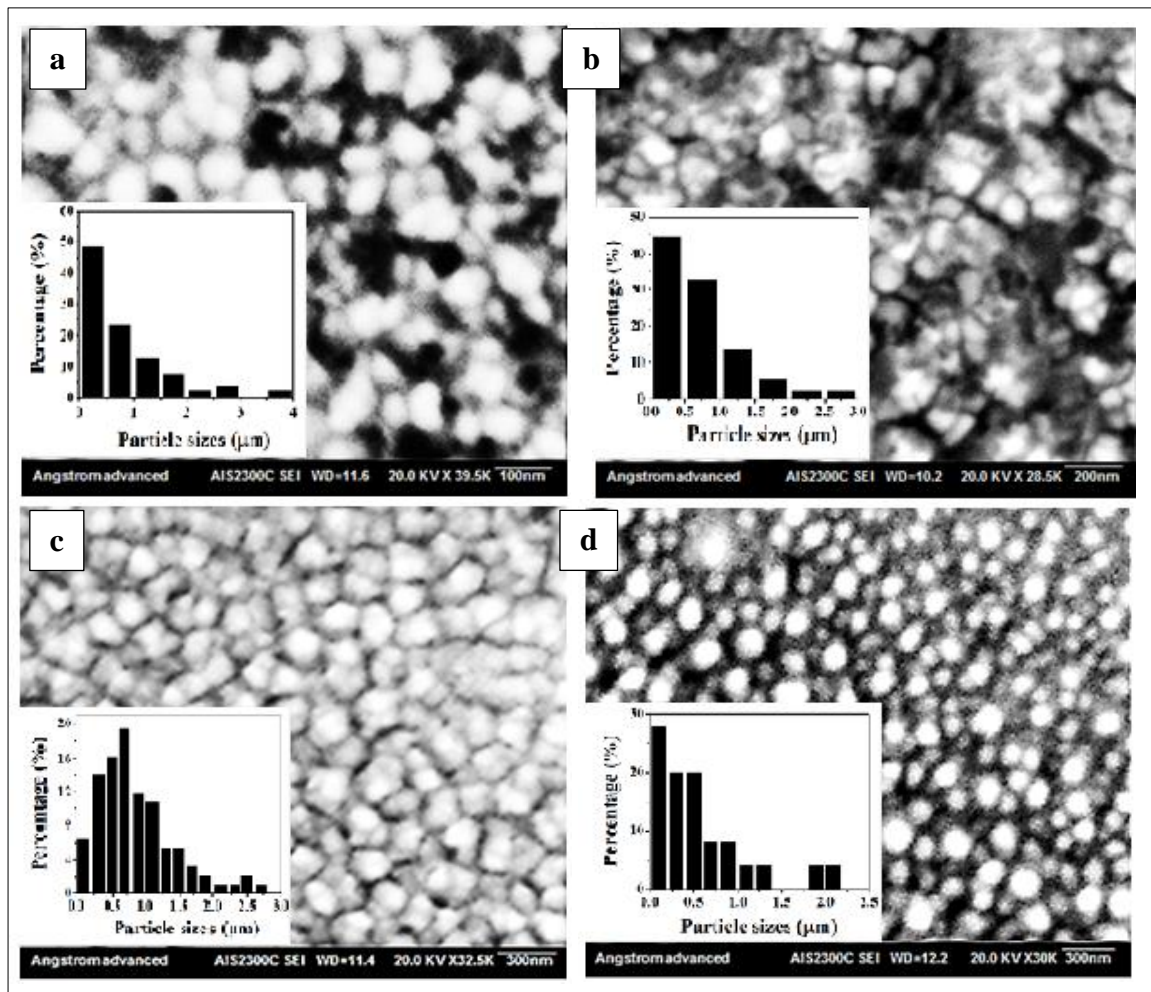


**Figure 5-** The SEM images and the statistical distribution of AuNPs sizes of PS/AuNPs structure surface deposited with  $\text{HAuCl}_4$  at concentrations of: a)  $10^{-2}$  M b)  $10^{-2}$  M diluted in HF c)  $5 \times 10^{-3}$  M d)  $5 \times 10^{-3}$  M diluted in HF.

Table- 3 shows the statistical distribution of AuNPs sizes.

**Table 3-** The statistical distribution of AuNPs size with their peak values

HAuCl <sub>4</sub> concentration (M)	Statistical distribution of Particle size of AuNPs(μm)	Statistical distribution peak(μm)
10 <sup>-2</sup>	(0.25-4)	0.25
10 <sup>-2</sup> + HF	(0.25-3)	0.25
5x10 <sup>-3</sup>	(0.25-2.75)	0.75
5x10 <sup>-3</sup> +HF	(0.25-2.25)	0.25

According to the results presented in Table-3 it can be seen obviously that the size of AuNPs clusters became smaller due to the important role of HF additive in destabilizing the AuNPs solution and reducing their tendency of aggregation. Also, the decreasing of HAuCl<sub>4</sub> concentration leads to smaller amounts of gold clusters which is confirmed by the statistical distribution mentioned earlier providing a better distribution for AuNPs solution on the surface of PS layer.

Figure-6 shows the EDX analysis that confirms the existence of AuNPs on the surface of PS/AuNPs structure.

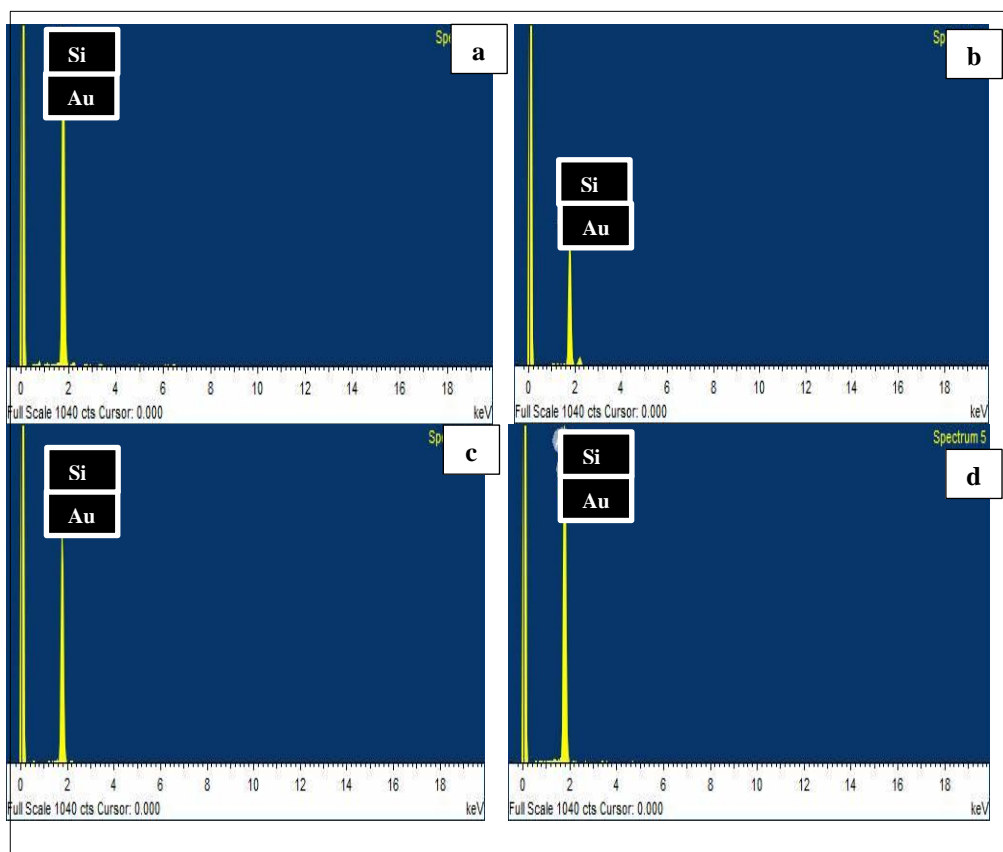


**Figure 6-** EDX analysis of AuNPs for PS/AuNPs structure surface deposited with HAuCl<sub>4</sub> at concentrations of: a) 10<sup>-2</sup> M b) 10<sup>-2</sup> M diluted in HF c) 5x10<sup>-3</sup> M d) 5x10<sup>-3</sup> M diluted in HF.

### 3.2) photoluminescence (PL) spectra

The PL spectra of bare PS samples before and after deposition process are presented in Figures-7 and 8 respectively. Also the numerical data obtained from PL measurements are shown in Table -4 .

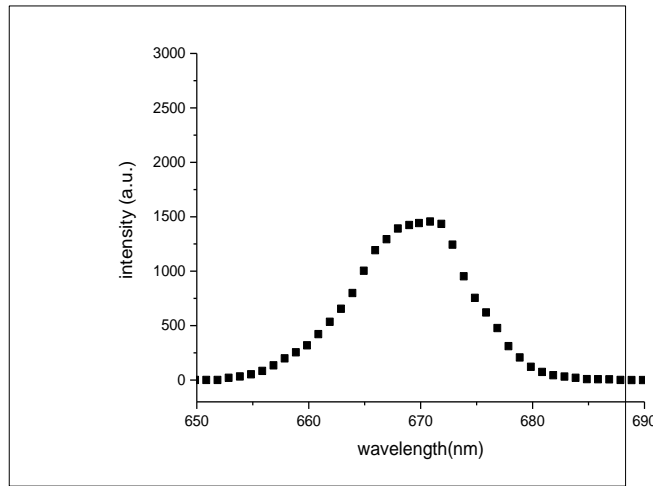


Figure 7- shows the PL spectra of bare PS.

Table 4- The PL emission wavelength, PS energy gap, and silicon nanosized.

PL emission wavelength (nm)	PL peak intensity (a.u)	PS energy gap(ev)	Si nano size(nm)
670	1465	1.85	3.3

The values of energy band gap of PS and silicon nanosized were calculated according to equation (5) [14]:

$$E_{g_{PS}} = E_{g_{Si}} + \frac{88.34}{L^{1.37}} \dots\dots\dots (5)$$

Where  $E_{g_{PS}}$  (eV) is the energy band gap of PS layer,  $E_{g_{Si}}$  (eV) is the energy band gap of bulk silicon (1.12) eV and  $L$  (nm) is nanocrystallite size.

In the same manner, Figure -8 indicates the PL spectra of PS/AuNPs structure samples deposited with  $HAuCl_4$  solution at concentrations of ( $10^{-2}M$ ,  $10^{-2} M$  diluted in HF,  $5 \times 10^{-3} M$ , and  $5 \times 10^{-3} M$  diluted in HF) respectively.

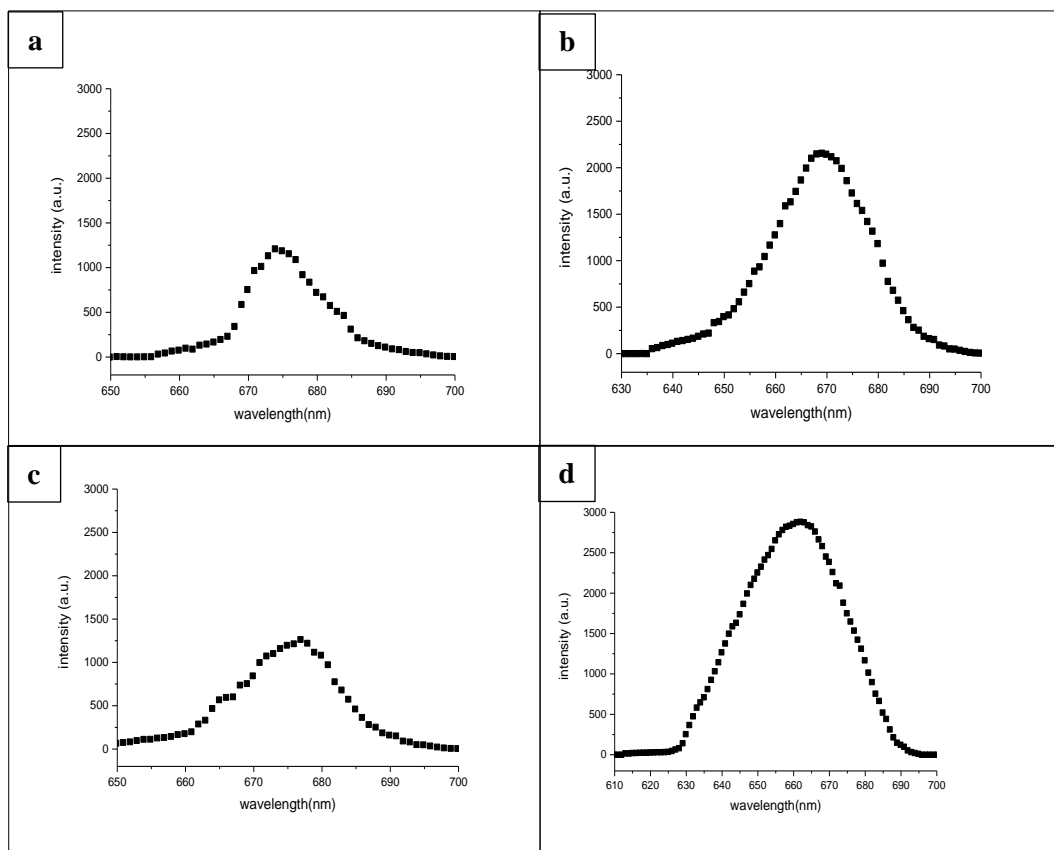


**Figure 8-** The PL spectra of PS/AuNPs structure surface deposited with HAuCl<sub>4</sub> at concentrations of: a)  $10^{-2}$  M b)  $10^{-2}$  M diluted in HF c)  $5 \times 10^{-3}$  M d)  $5 \times 10^{-3}$  M diluted in HF.

The obtained results from of PL spectra for PS/AuNPs structure are presented in Table-5.

**Table 5-** The PL wavelength and PL peak intensity as a function of AuNPs concentration

AuNPs concentration(M)	PL wavelength (nm)	PL peak intensity (a.u.)
$10^{-2}$	<b>673</b>	<b>1210</b>
$10^{-2}$ +HF	<b>668</b>	<b>2155</b>
$5 \times 10^{-3}$	<b>676</b>	<b>1265</b>
$5 \times 10^{-3}$ +HF	<b>670</b>	<b>2883</b>

The variations of PL spectra as illustrated in Table-5 can be explained as follows:

The enhancement process of PL intensity is related to the role of the AuNPs in the reduction of the non-radiative recombination centers (dangling bonds), the reduction of these sites will lead to increase the radiation recombination between electrons and holes in PS matrix which is also confirmed by the statistical distribution measurements of particles sizes. The improvement in the photoluminescence spectrum of PS/AuNPs may be reduced due to the contribution of HF acid in destabilizing the colloidal gold which is characterized by localized surface Plasmon resonance (LSPR) that yields to resonant coupling with electronic excitation of PS and inhibit the non-radiative Auger recombination. This means that the intensity of PL spectra is highly dependent on the concentration of AuNPs and their size distribution and the morphology of their clusters.

The quenching of PL intensity after treating PS layer with AuNPs is related to the sizes of AuNPs because without adding HF acid to the immersion solution the sizes of AuNPs have higher values comparing with that after adding HF acid. The energy of incident photon is dissipated by absorption

and far-field radiation which is formed by scattering, where larger AuNPs are more expected to reduce PL spectra and smaller AuNPs are more expected to improve PL or fluorophore because the scattering component is dominant over absorption.

#### 4) Conclusion

The growth of AuNPs on the surface of PS was successfully obtained using a cost effective and simple immersion plating method. The SEM images showed different sizes of gold clusters on the surface of PS due to the effect of adding HF acid as a diluting agent that controls the growth mechanism of AuNPs.

Efficient PL improvement was obtained at the lowest sizes of AuNPs without the aggregation of AuNPs cluster form.

Our outcomes open the possibility of fabricating nanostructured substrates by means of simple preparation procedures with a high reproducible form, acceptable uniformity, and suitability for monitoring environmental pollution levels and gas sensing applications.

#### References

1. Juraj Dian, Tomas Chvojka, Vladimir Vrkoslav, and Ivan Jelinek. **2005**. photoluminescence quenching of porous silicon in gas and liquid phases-the role of dielectric quenching and capillary condensation effects, *phys. Stat. sol. (c)* 2, No.9, pp: 3481-3485/DOI 10.1002/pssc.200461227.
2. Asmiet Ramizy, Z. Hassan, Khalid Omar. **2011**. Porous silicon nanowires fabricated by electrochemical and laser-induced etching, *Mater Sci: Mater Electron*, 22, pp:717–723. DOI 10.1007/s10854-010-0199-3.
3. Hayder, J. Adawya, M. Alwan Alwan, A. Jabbar Allaa. **2016**. Optimizing of porous silicon morphology for synthesis of silver nanoparticles, *Microporous and Mesoporous Materials*, 227, pp: 152-160.
4. Petra Granitzer and Klemens Rumpf. **2010**. Porous Silicon—A Versatile Host Material, *Materials*, 3, pp: 943-998; DOI: 10.3390/ma3020943.
5. Saakshi Dhanekar, Swati Jain. **2013**. Porous silicon biosensor: Current status, *Biosensors and Bioelectronics*, 41, pp: 54–64.
6. Meddeb Hosny, Dimassi Wissem, Haddadi Ikbel, and Ezzaouia Hatem. **2014**. Influence of Gold Nanoparticles Deposition on Porous Silicon Properties, *Sensors & Transducers*, 27, Special Issue, pp: 202-208.
7. Montassar Billeh Bouzouraa, Mehdi Rahmani, Mohamed-Ali Za\_bi, Nathalie Lorrain, Lazhar Haji, et al. **2013**. Optical study of annealed cobalt-porous silicon nanocomposites. *Journal of Luminescence*, Elsevier, 2013, 143, pp: 521-525. <10.1016/j.jlumin.05.050>. <hal-00840826>
8. Douglas A.Skoog, Donald M.West, F.James Holler & Stanley R.Crouch. **2004**. *Fundamentals of analytical chemistry*, Thomson, United states of America, eight edition.
9. Jalil (Kamran) Khajehpour Tadvani. **2013**. Gold nanothorns – macroporous silicon hybrid structure: a simple and ultrasensitive platform for SERS, Ph.D. thesis, School of Applied Sciences and Engineering Faculty of Science Monash University, Australia.
10. Kirk-Otmer, *Encyclopedia of Chemical Technology*”, Third Edition, Vol. I, Wiley-Interscience, New York, V 3, pp: 510-512; V. 8, pp: 738-750.826-869; V. 15, pp: 241-308; V. 20, pp: 38-42; V. 10, pp: 247-250, V. 11, pp: 988-994, V: 14, pp: 694.
11. Narender Budhiraja, Ashwani Sharma, Sanjay Dahiya, Rajesh Parmar, & Viji Vidyadharan. **2013**. Synthesis and optical characteristics of silver nanoparticles on different substrates", *International Letters of Chemistry, Physics and Astronomy*, 19, pp 80-88.
12. Alwan M. Alwan, Adawya J.Hayder, Allaa A. Jabbar. **2015**. Study on morphological and structural properties of silver plating on laser etched silicon. *Surface & Coatings Technology*, 283, pp: 22–28.
13. Anup Kr Kalita and Sanjib Karmakar,. **2016**. Effect On Particle Size And Microstrain Due To Iron Doping On Zno Nanoparticle Prepared By Wet Chemical Method. *International Journal of Scientific Reseach*, 5(2) , pp:654-655.
14. Amna A. Salman, Fatima I. Sultan, and Uday M. Nayef. **2012**. Structural, Chemical and Morphological of Porous Silicon Produced by Electrochemical Etching, *Eng. &Tech. Journal* , 30 (5), pp: 855-868.